Filomat 38:12 (2024), 4187–4207
https://doi.org/10.2298/FIL2412187W

Published by Faculty of Sciences and Mathematics,
University of Niš, Serbia
Available at: http://www.pmf.ni.ac.rs/filomat

Structure-preserving numerical methods for the two dimensional nonlinear fractional wave equation

Longbin Wu[a], Qiang Ma[a,*], Xiaohua Ding[a]

[a]*Department of Mathematics, Harbin Institute of Technology at Weihai, Shandong, P.R.China*

Abstract. This paper introduces the structure-preserving numerical methods for the two dimensional nonlinear fractional wave equation. By using the variational principle with fractional Laplace, the equation is transformed into a Hamiltonian system with symplectic and multi-symplectic structure, and they show the corresponding conservation laws. Then a numerical method is proposed with the Fourier pseudospectral method in space and midpoint method in time. It is proved that the proposed numerical method preserves the corresponding conservation laws in the discrete sense. Furthermore, one investigates energy errors of fully discrete schemes, and discusses convergence of the proposed schemes which are second-order accuracy in time and spectral accuracy in space. Finally, the validity and accuracy of the theoretical results are verified by several numerical examples.

1. Introduction

The nonlinear wave equation is an important class of mathematical models in some scientific fields like acoustics, electromagnetism and fluid mechanics, etc. As we all know, one key feature of the nonlinear wave equation is that it can be written as a Hamiltonian system. The Hamiltonian system can describe all real physical processes with negligible dissipation. In fact, the exact solution of nonlinear Hamiltonian system can not be obtained generally. Considering the need of scientific calculation and computer simulation, it is necessary to construct an effective numerical method to simulate the behavior of the solution of Hamiltonian system by computer. In the current researches of numerical methods, it is generally required that the basic characteristics of the original problem should be preserved as much as possible after discretization [8], that is, the discretization should be carried out in the unified framework of the original problem as much as possible. So for some partial differential equations (PDEs) which can be transformed into Hamiltonian system, it is very important to design a numerical method which can satisfy the symplecticity of the original system, because it has conspicuous ability to preserve the geometric properties of phase space for a long time [9, 11, 20] and has good numerical stability. In general, symplectic and multi-symplectic structure are important approaches to the structure-preserving schemes for solving nonlinear Hamiltonian PDEs [18, 32, 33]. For classical nonlinear wave equation, a lot of symplectic and multi-symplectic methods have been constructed [2, 13, 23, 24, 28].

2020 *Mathematics Subject Classification*. 65M12, 65M70
Keywords. two dimensional nonlinear fractional wave equation, multi-symplectic method, conservation laws, convergence
Received: 24 February 2022; Revised: 28 October 2023; Accepted: 16 November 2023
Communicated by Marko Nedeljkov
Research supported by the Natural Science Foundation of Shandong Province of China (No. ZR2020MA050).
* Corresponding author: Qiang Ma
Email addresses: wlb@hit.edu.cn (Longbin Wu), hitmaqiang@hit.edu.cn (Qiang Ma), mathdxh@hit.edu.cn (Xiaohua Ding)

In recent years, the development of fractional caculus has opened new perspectives in sciences and engineering [12, 15, 17, 25]. In particular, the nonlinear fractional equation has attracted extensive attention of scholars, such as fractional Schrödinger equations, fractional wave equations and so on. As a variety of wave phenomena in nature, including long wave and short wave, such as sound wave, light wave and water wave, can be described by the corresponding wave equation, the specific form of wave function and its corresponding energy can be obtained, so as to understand the wave propagation and some properties. Therefore, nonlinear fractional wave equation becomes an important equation in physics. It describes the law of micro object moving at high speed, which deepens the understanding of micro world and provides a theoretical basis for dealing with the problem of atomic structure systematically and quantitatively. In this paper, we consider the following nonlinear fractional wave equation

$$\begin{cases} \partial_{tt}u + (-\Delta)^{\frac{\alpha}{2}}u + G'(u) = 0, \quad t \in [0, T], \\ u(\mathbf{x}, 0) = u_0(\mathbf{x}), \quad \mathbf{x} \in \Omega, \\ u_t(\mathbf{x}, 0) = u_1(\mathbf{x}), \end{cases} \tag{1}$$

where $\mathbf{x} = (x, y)$, $\Omega = [a, b] \times [a, b]$, $1/2 < \alpha < 1$, $G : \mathbb{R} \to \mathbb{R}$ is a nonlinear and smooth function, (1) is prescribed with either homogeneous Dirichlet (inhomogeneous Dirichlet) or periodic boundary conditions. For other boundary conditions, it is difficult to determine whether the equation still has symplectic and multi-symplectic structures. In this paper, we mainly consider the case of periodic boundary. The fractional derivative $(-\Delta)^{\frac{\alpha}{2}}$ are defined as a pseudo-differential operator with its symbol in the Fourier space. For the bounded interval Ω with periodic boundary conditions, it can be defined by Fourier series [1]

$$-(-\Delta)^{\frac{\alpha}{2}}u(\mathbf{x}, t) = -\sum_{l_1, l_2 \in \mathbb{Z}} |\xi_{l_1}^2 + \xi_{l_2}^2|^{\frac{\alpha}{2}} \hat{u}_l e^{\mathrm{i}\xi_{l_1}(x-a) + \mathrm{i}\xi_{l_2}(y-a)},$$

where $\xi_{l_i} = \frac{2l_i\pi}{b-a}$, and $\hat{u}_l$ is Fourier coefficient and is given by

$$\hat{u}_l = \frac{1}{(b-a)^2} \int_\Omega u(\mathbf{x}, t) e^{-\mathrm{i}\xi_{l_1}(x-a) - \mathrm{i}\xi_{l_2}(y-a)} d\mathbf{x}.$$

In general, it notices that geometric structures for nonlinear Hamiltonian PDEs have had the development of numerical methods, which systematically incorporate qualitative features of the underlying problem into their structure. Various invariant-preserving numerical methods have been developed for computing classical nonlinear wave equation, including the finite difference method [6, 14, 16], spectral or collocation method [3–5], finite element method [22, 26], etc.

For the study of fractional differential equation with geometric structures, it is also important to develop structure-preserving numerical methods. In [29], authors give variational principle of the fractional Laplacian and show that the fractional Schrödinger equation can be reformulated as a Hamiltonian system with a symplectic structure. Then using Fourier pseudospectral method in space, it is proved that the discrete fractional Hamiltonian system satisfy the corresponding symplectic or other conservation laws in the discrete sense. Xiao and Wang [31] give a fourth-order central difference method in space for fractional Schrödinger equation, and the semi-discretization system is shown to be a finite dimension Hamiltonian system. Moreover, they apply midpoint method in the temporal for the Hamiltonian system to preserve some properties. Furthermore, Fei et al. [7] give the convergence order and error estimate of the multi-symplectic Hamiltonian system of fractional Schrödinger equation. Recently, Wang [27] gives the symplectic-preserving Fourier spectral scheme for space fractional KGS equations. However, there are few studies on symplectic and multi-symplectic for nonlinear fractional wave equations. And we notice that the analysis of convergence is almost absent for multi-symplectic methods. Based on the above main motivation, we consider the symplectic and multi-symplectic Hamiltonian structure of two dimensional nonlinear fractional wave equations and the convergence of numerical methods. The main contributions reside in the following aspects.

- It gives symplectic and multi-symplectic structure for the two dimensional nonlinear fractional wave equation, and a numerical method is proposed with the Fourierpseudospectral method in space and midpoint method in time.

- Some numerical theoretical analysis are given, including discrete conservation laws, energy errors and convergence.
- There is almost no convergence analysis of the multi-symplectic method, so the convergence analysis of the multi-symplectic method is given in this paper.
- Several numerical examples illustrate the efficiency and accuracy of the numerical scheme.

The present paper is organized as follows. In section 2, one gives symplectic and multi-symplectic Hamiltonian formulations and their conservation laws for the two dimensional nonlinear fractional wave equation. Section 3 shows that Fourier pseudospectral method in the spatial and given the conservation law of the corresponding semi-discrete scheme. Then the fully discrete symplectic and multi-symplectic schemes are obtained by using the midpoint method in the temporal, and it is presented error estimates of energy. Finally, conservation laws of the fully discrete schemes are strictly proved. Section 4 is devoted to a rigorous convergence analysis for the multi-symplectic Fourier pseudospectral scheme. In section 5, the validity and accuracy of the theoretical results are verified by some numerical examples. In the end, we close this paper of concluding remarks.

2. Symplectic and multi-symplectic Hamiltonian formulations and conservation laws

This section gives symplectic and multi-symplectic Hamiltonian formulations and their conservation laws for the nonlinear fractional wave equation. A lemma first is given with respect to the fractional Laplacian.

Lemma 2.1. *[30] Letting u be a periodic function, then it holds*

$$-(-\Delta)^{\frac{\alpha}{2}}u = \mathcal{L}^2 u := \mathcal{L}(\mathcal{L}u), \tag{2}$$

where $\mathcal{L}u = \sum_{l_1,l_2\in\mathbb{Z}} \mathrm{i}\begin{pmatrix} \xi_{l_1} \\ \xi_{l_2} \end{pmatrix} |\xi_{l_1}^2 + \xi_{l_2}^2|^{\frac{\alpha-2}{4}} \hat{u}_l e^{\mathrm{i}\xi_{l_1}(x-a)+\mathrm{i}\xi_{l_2}(y-a)}$. *In particular, when* $\alpha = 2$, *the operator* $\mathcal{L}$ *reduces to the gradient operator.*

For writing convenience, defined $\mathcal{L} := (\mathcal{L}_x \ \ \mathcal{L}_y)^T$, so $-(-\Delta)^{\frac{\alpha}{2}} = \mathcal{L}_x^2 + \mathcal{L}_y^2$.

2.1. Symplectic Hamiltonian formulation

The nonlinear fractional wave equation (1) has a symplectic structure, when $\alpha = 2$ is a well-known classical Hamiltonian structure. Introducing $v = u_t$, a pair of equations can be rewrite (1) as

$$\begin{cases} u_t = v, \\ v_t = -(-\Delta)^{\frac{\alpha}{2}}u - G'(u). \end{cases} \tag{3}$$

By the fractional variational calculus formula [29], one obtains that system (3) is an infinite-dimensional Hamiltonian system

$$\frac{d}{dt}\begin{pmatrix} u \\ v \end{pmatrix} = J\delta H, \ \ J = \begin{pmatrix} 0 & 1 \\ -1 & 0 \end{pmatrix}, \tag{4}$$

where the Hamiltonian functional H is

$$H = \int_\Omega \Big(\frac{1}{2}(v^2 + ((-\Delta)^{\frac{\alpha}{4}}u)^2) + G(u)\Big) d\mathbf{x},$$

which is invariant with respect to time. The Hamiltonian system (4) satisfies the symplectic conservation law

$$\frac{d}{dt}\int_\Omega (du \wedge dv) d\mathbf{x} = 0, \tag{5}$$

where $\wedge$ denotes the wedge product.

2.2. Multi-symplectic Hamiltonian formulation

The nonlinear fractional wave equation can also be formulated as a multi-symplectic Hamiltonian system which possesses a local multi-symplectic conservation law. Denoting $v = u_t$, $w_1 = \mathcal{L}_x u$, $w_2 = \mathcal{L}_y u$ and one rewrites (1)

$$\begin{cases} -v_t + \mathcal{L}_x w_1 + \mathcal{L}_y w_2 = G'(u), \\ u_t = v, \\ -\mathcal{L}_x u = -w_1, \\ -\mathcal{L}_y u = -w_2. \end{cases} \tag{6}$$

The system (6) can be rewritten as the multi-symplectic Hamiltonian system

$$Mz_t + K_1(\mathcal{L}_x z) + K_2(\mathcal{L}_y z) = \nabla_z S(z), \tag{7}$$

where $z = (u, v, w_1, w_2)^T$, M, K are the skew-symmetry matrices

$$M = \begin{pmatrix} 0 & -1 & 0 & 0 \\ 1 & 0 & 0 & 0 \\ 0 & 0 & 0 & 0 \\ 0 & 0 & 0 & 0 \end{pmatrix}, \quad K_1 = \begin{pmatrix} 0 & 0 & 1 & 0 \\ 0 & 0 & 0 & 0 \\ -1 & 0 & 0 & 0 \\ 0 & 0 & 0 & 0 \end{pmatrix}, \quad K_2 = \begin{pmatrix} 0 & 0 & 0 & 1 \\ 0 & 0 & 0 & 0 \\ 0 & 0 & 0 & 0 \\ -1 & 0 & 0 & 0 \end{pmatrix},$$

and the Hamiltonian function

$$S(z) = \frac{1}{2}(v^2 - w^2) + G(u).$$

Theorem 2.2. *The system* (7) *satisfies the multi-symplectic conservation law*

$$\partial_t \omega + \kappa_{\mathbf{x}} = 0, \tag{8}$$

where

$$\omega = \frac{1}{2} dz \wedge M dz, \quad \kappa_{\mathbf{x}} = dz \wedge K_1 \mathcal{L}_x dz + dz \wedge K_2 \mathcal{L}_y dz.$$

Proof. Taking differential on both sides of (7) to get

$$M dz_t + K_1 d(\mathcal{L}_x z) + K_2 d(\mathcal{L}_y z) = S_{zz} dz.$$

It is obtained by the wedge product of the above formula and dz

$$dz \wedge M dz_t + dz \wedge K_1 d(\mathcal{L}_x z) + dz \wedge K_2 d(\mathcal{L}_y z) = dz \wedge S_{zz} dz.$$

Because S_{zz} is symmetric, $dz \wedge S_{zz} dz = 0$,

$$dz \wedge M dz_t + dz \wedge K_1 d(\mathcal{L}_x z) + dz \wedge K_2 d(\mathcal{L}_y z) = 0.$$

Since M, K_1 and K_2 are skew-symmetric matrices, it has

$$dz_t \wedge M dz + d(\mathcal{L}_x z) \wedge K_1 dz + d(\mathcal{L}_y z) \wedge K_2 dz = 0.$$

So

$$\partial_t \omega + \frac{1}{2}(\mathcal{L}_x dz \wedge K_1 dz + dz \wedge K_1 \mathcal{L}_x dz + \mathcal{L}_y dz \wedge K_2 dz + dz \wedge K_2 \mathcal{L}_y dz) = 0.$$

K_1 and K_2 are skew-symmetric matrices, $\mathcal{L}_x dz \wedge K_1 dz = dz \wedge K_1 \mathcal{L}_x dz$, $\mathcal{L}_y dz \wedge K_2 dz = dz \wedge K_2 \mathcal{L}_y dz$, so

$$\partial_t \omega + dz \wedge K_1 \mathcal{L}_x dz + dz \wedge K_2 \mathcal{L}_y dz = 0.$$

Thus the proof is completed. □

Integrating (8) over Ω and using the periodic boundary conditions, one has

$$0 = \int_\Omega (\partial_t \omega + \kappa_{\mathbf{x}}) d\mathbf{x} = \int_\Omega \partial_t \omega d\mathbf{x} = \frac{d}{dt}\int_\Omega (du \wedge dv) d\mathbf{x},$$

which is just the symplectic conservation law (5).

Theorem 2.3. *The system* (7) *satisfies the local energy conservation law*

$$\partial_t E + F_{\mathbf{x}} = 0,$$

where

$$E = S(z) - \frac{1}{2}\left(z^T K_1(\mathcal{L}_x z) + z^T K_2(\mathcal{L}_y z)\right), \ \ F_{\mathbf{x}} = \frac{1}{2}\left((\mathcal{L}_x z)^T K_1 z_t + z^T K_1 (\mathcal{L}_x z)_t + (\mathcal{L}_y z)^T K_2 z_t + z^T K_2 (\mathcal{L}_y z)_t\right).$$

Proof. Noting that

$$\begin{aligned}\partial_t E &= z_t^T \nabla_z S(z) - \frac{1}{2} z_t^T K_1(\mathcal{L}_x z) - \frac{1}{2} z^T K_1(\mathcal{L}_x z)_t - \frac{1}{2} z_t^T K_2(\mathcal{L}_y z) - \frac{1}{2} z^T K_2(\mathcal{L}_y z)_t \\ &= z_t^T M z_t + z_t^T K_1(\mathcal{L}_x z) + z_t^T K_2(\mathcal{L}_y z) - \frac{1}{2} z_t^T K_1(\mathcal{L}_x z) - \frac{1}{2} z^T K_1(\mathcal{L}_x z)_t - \frac{1}{2} z_t^T K_2(\mathcal{L}_y z) - \frac{1}{2} z^T K_2(\mathcal{L}_y z)_t \\ &= \frac{1}{2} z_t^T K_1(\mathcal{L}_x z) - \frac{1}{2} z^T K_1(\mathcal{L}_x z)_t + \frac{1}{2} z_t^T K_2(\mathcal{L}_y z) - \frac{1}{2} z^T K_2(\mathcal{L}_y z)_t.\end{aligned}$$

Similarly,

$$F_{\mathbf{x}} = -\frac{1}{2} z_t^T K_1(\mathcal{L}_x z) + \frac{1}{2} z^T K_1(\mathcal{L}_x z)_t - \frac{1}{2} z_t^T K_2(\mathcal{L}_y z) + \frac{1}{2} z^T K_2(\mathcal{L}_y z)_t.$$

So $\partial_t E + F_{\mathbf{x}} = 0$. □

Theorem 2.4. *The system* (7) *satisfies the local momentum conservation law in each of the sub-direction*

$$\begin{aligned}&\partial_t I_x + \mathcal{L}_x V_x + \mathcal{L}_y \widetilde{V_{xy}} = 0,\\ &\partial_t I_y + \mathcal{L}_y V_y + \mathcal{L}_x \widetilde{V_{yx}} = 0,\end{aligned}$$

where

$$\begin{aligned}&I_x = \frac{1}{2} z^T M(\mathcal{L}_x z), \ \ V_x = S(z) - \frac{1}{2}\left(z^T M z_t + z^T K_2(\mathcal{L}_y z)\right), \ \ \widetilde{V_{xy}} = \frac{1}{2} z^T K_2(\mathcal{L}_x z),\\ &I_y = \frac{1}{2} z^T M(\mathcal{L}_y z), \ \ V_y = S(z) - \frac{1}{2}\left(z^T M z_t + z^T K_1(\mathcal{L}_x z)\right), \ \ \widetilde{V_{yx}} = \frac{1}{2} z^T K_1(\mathcal{L}_y z).\end{aligned}$$

Proof. We only prove the local momentum conservation law in the x-axis direction, and the y-axis can be obtained in the same way. It is obtained by multiplying system (7) left by $(\mathcal{L}_x z)^T$

$$(\mathcal{L}_x z)^T M z_t + (\mathcal{L}_x z)^T K_1(\mathcal{L}_x z) + (\mathcal{L}_x z)^T K_2(\mathcal{L}_y z) = (\mathcal{L}_x z)^T \nabla_z S(z).$$

Since K_1 is skew-symmetric matrix

$$(\mathcal{L}_x z)^T M z_t + (\mathcal{L}_x z)^T K_2(\mathcal{L}_y z) = (\mathcal{L} z)^T \nabla_z S(z).$$

It notices that

$$\partial_t I = \frac{1}{2}\left(z_t^T M(\mathcal{L} z) + z^T M(\mathcal{L} z)_t\right),$$

so

$$\partial_t I_x + \mathcal{L}_x V_x + \mathcal{L}_y \widetilde{V_{xy}} = \frac{1}{2}\left(z_t^T M(\mathcal{L}_x z) + z^T M(\mathcal{L}_x z)_t\right) + (\mathcal{L}_x z)^T \nabla_z S(z) - \frac{1}{2}\left((\mathcal{L}_x z)^T M z_t + z^T M(\mathcal{L}_x z)_t\right)$$
$$- \frac{1}{2}\left((\mathcal{L}_x z)^T K_2(\mathcal{L}_y z) + z^T K_2(\mathcal{L}_x \mathcal{L}_y z)\right) + \frac{1}{2}\left((\mathcal{L}_y z)^T K_2(\mathcal{L}_x z) + z^T k_2(\mathcal{L}_x \mathcal{L}_y z)\right)$$
$$= (\mathcal{L} z)^T \nabla_z S(z) - (\mathcal{L}_x z)^T M z_t + (\mathcal{L}_x z)^T K_2(\mathcal{L}_y z) = 0.$$

□

Remark 2.5. *When $\alpha = 2$, the above conservation laws will reduce to the standard local conservation laws in* [19] *for the classical wave equation.*

3. Structure-preserving numerical methods

In this section, we present structure-preserving numerical methods. First of all, the spatial discretization is give. Since fractional Laplace and $\mathcal{L}$ operator are defined by symbols in the Fourier space, they can naturally be approximated by the Fourier pseudospectral method [21]. Firstly, the numerical solution is constructed by interpolating trigonometric polynomials of the solution at collocation points. Second, the fractional derivative is approximated in frequency space.

For the convenience of narration, some notations are introduced. Similarly, for two given positive even integer N_x, N_y, one considers the set of points $x_l = a + (b-a)l/N_x$, $l = 0, 1, \cdots, N_x - 1$ and $y_m = a + (b-a)m/N_y$, $m = 0, 1, \cdots, N_y - 1$ are referred as space collocation points. So

$$I_N u(x, y) = \sum_{l_1=-\frac{N_x}{2}}^{\frac{N_x}{2}} \sum_{l_2=-\frac{N_y}{2}}^{\frac{N_y}{2}} \tilde{u}_{l_1 l_2} e^{\mathrm{i}\xi l_1(x-a)+\mathrm{i}\xi l_2(y-a)},$$

with

$$\tilde{u}_{l_1 l_2} = \frac{1}{N_x N_y c_{l_1} c_{l_2}} \sum_{l=0}^{N_x-1} \sum_{m=0}^{N_y-1} u(x_l, y_m) e^{-\mathrm{i}\xi l_1(x_l-a)-\mathrm{i}\xi l_2(y_m-a)},$$

where $\xi = 2\pi/(b-a)$, $c_{l_1} = 1$ when $|l_1| < N_x/2$, $c_{l_1} = 2$ when $|l_1| = N_x/2$ and $c_{l_2} = 1$ when $|l_2| < N_y/2$, $c_{l_2} = 2$ when $|l_2| = N_y/2$. So $I_N u(x_l, y_m) = u(x_l, y_m)$ for $l = 0, 1, \cdots, N_x - 1$, $m = 0, 1, \cdots, N_y - 1$. Then $-(-\Delta)^{\frac{\alpha}{2}} I_N u(x, y)$, $\mathcal{L}_x I_N u(x, y)$ and $\mathcal{L}_y I_N u(x, y)$ can be defined by Fourier series

$$-(-\Delta)^{\frac{\alpha}{2}} I_N u(x_j, y_{k},) = -\sum_{l_1=-\frac{N_x}{2}}^{\frac{N_x}{2}} \sum_{l_2=-\frac{N_y}{2}}^{\frac{N_y}{2}} ((\xi l_1)^2 + (\xi l_2)^2)^{\frac{\alpha}{2}} \tilde{u}_{l_1 l_2} e^{\mathrm{i}\xi l_1(x_j-a)+\mathrm{i}\xi l_2(y_k-c)} = (D_2^\alpha \mathbf{u})_{jk}, \tag{9}$$

$$\mathcal{L}_x I_N u(x_j, y_k) = \mathrm{i} \sum_{l_1=-\frac{N_x}{2}}^{\frac{N_x}{2}} \sum_{l_2=-\frac{N_y}{2}}^{\frac{N_y}{2}} \xi l_1((\xi l_1)^2 + (\xi l_2)^2)^{\frac{\alpha-2}{4}} \tilde{u}_{l_1 l_2} e^{\mathrm{i}\xi l_1(x_j-a)+\mathrm{i}\xi l_2(y_k-c)} = ({}_{1x}D^\alpha \mathbf{u})_{jk}. \tag{10}$$

$$\mathcal{L}_y I_N u(x_j, y_k) = \mathrm{i} \sum_{l_1=-\frac{N_x}{2}}^{\frac{N_x}{2}} \sum_{l_2=-\frac{N_y}{2}}^{\frac{N_y}{2}} \xi l_2((\xi l_1)^2 + (\xi l_2)^2)^{\frac{\alpha-2}{4}} \tilde{u}_{l_1 l_2} e^{\mathrm{i}\xi l_1(x_j-a)+\mathrm{i}\xi l_2(y_k-c)} = ({}_{1y}D^\alpha \mathbf{u})_{jk}, \tag{11}$$

where $\mathbf{u} = (u_{00}, u_{01}, \cdots, u_{0N_y-1}, \cdots, u_{N_x-1N_y-1})^T$. According to (9) and (10), D_2^α, ${}_{1x}D^\alpha$ and ${}_{1y}D^\alpha$ are $N \times N$ matrices, and whose elements are refferred to in Ref.[30]. Let $l_i = -l_i$, $i = 1, 2$, it is easy to know D_2^α is a symmetric matrix and ${}_{1x}D^\alpha$ and ${}_{1y}D^\alpha$ are skew-symmetric matrices.

3.1. Symplectic discretization method

Using the matrix D_2^α, a semi-discrete system is obtained by the Fourier pseudospectral discretization in space for the system (3)

$$\begin{cases} \frac{d}{dt}u_{lm} = v_{lm}, \\ \frac{d}{dt}v_{lm} - (D_2^\alpha \mathbf{u})_{lm} + G'(u_{lm}) = 0, \end{cases} \tag{12}$$

where $l = 0, \cdots, N-1,\ \mathbf{u} = (u_{00}, u_{01}, \cdots, u_{0N_y-1}, \cdots, u_{N_x-1N_y-1})^T$. So the semi-discrete system (12) is a finite dimensional Hamiltonian system

$$\begin{cases} \frac{du}{dt} = \nabla_v H_h, \\ \frac{dv}{dt} = -\nabla_u H_h, \end{cases} \tag{13}$$

with the Hamiltonian function

$$H_h(\mathbf{u}, \mathbf{v}) = \frac{1}{2}\left(\mathbf{v}^T\mathbf{v} - \mathbf{u}^T D_2^\alpha \mathbf{u}\right) + \sum_{l=0}^{N_x-1}\sum_{m=0}^{N_y-1} G(u_{lm}).$$

In addition, the Hamiltonian system (13) is the symplectic Fourier pseudospectral discretization of the nonlinear fractional wave equation and satisfies the semi-discrete symplectic conservation law

$$\frac{d}{dt}\sum_{l=0}^{N_x-1}\sum_{m=0}^{N_y-1}(du_{lm} \wedge dv_{lm}) = 0.$$

It is worthy of note that (13) is a semi-discrete Hamiltonian system, one can adopt implicit midpoint method to (13).

$$\begin{cases} \frac{u_{lm}^{n+1} - u_{lm}^n}{\tau} = v_{lm}^{n+\frac{1}{2}}, \\ \frac{v_{lm}^{n+1} - v_{lm}^n}{\tau} - (D_2^\alpha \mathbf{u}^{n+\frac{1}{2}})_{lm} + G'(u_{lm}^{n+\frac{1}{2}}) = 0, \end{cases} \tag{14}$$

where $n = 1, 2, \cdots, N_t$, $\tau = T/N_t$, $u_{lm}^{n+\frac{1}{2}} = (u_{lm}^n + u_{lm}^{n+1})/2$, $v_{lm}^{n+\frac{1}{2}} = (v_{lm}^n + v_{lm}^{n+1})/2$. So the system (13) is integrated with a symplectic integrator, the scheme (14) satisfies the full-discrete symplectic conservation law

$$\frac{\sum_{l=0}^{N_x-1}\sum_{m=0}^{N_y-1}\left(du_{lm}^{n+1} \wedge dv_{lm}^{n+1} - du_{lm}^n \wedge dv_{lm}^n\right)}{\tau} = 0, \tag{15}$$

or equivalently,

$$\sum_{l=0}^{N_x-1}\sum_{m=0}^{N_y-1}(du_{lm}^{n+1} \wedge dv_{lm}^{n+1}) = \sum_{l=0}^{N_x-1}\sum_{m=0}^{N_y-1}(du_{lm}^n \wedge dv_{lm}^n).$$

So the scheme (14) preserves symplectic conservation laws in the fully discrete sense. However, it can not preserve the global and local energy conservation laws in general. Therefore, it is essential to analyze the error in energy conservation law for the fully discrete scheme (14).

Denoting $h = 2\pi/(b-a)$ and letting $(\mathbf{u}, \mathbf{v})$ be the solution of the symplectic Fourier pseudospectral method, and $H_h^{n+\frac{1}{2}}$ as follows

$$H_h^{n+\frac{1}{2}}(\mathbf{u}, \mathbf{v}) = \frac{h^2}{2}\left((\mathbf{v}^{n+\frac{1}{2}})^T\mathbf{v}^{n+\frac{1}{2}} - (\mathbf{u}^{n+\frac{1}{2}})^T D_2^\alpha \mathbf{u}^{n+\frac{1}{2}}\right) + h^2\sum_{l=0}^{N_x-1}\sum_{m=0}^{N_y-1} G(u_{lm}^{n+\frac{1}{2}}),$$

and equivalent to

$$H_h^{n+\frac{1}{2}}(\mathbf{u},\mathbf{v}) = \frac{h^2}{2}\left((\mathbf{v}^{n+\frac{1}{2}},\mathbf{v}^{n+\frac{1}{2}})_h - (\mathbf{u}^{n+\frac{1}{2}}, D_2^{\alpha}\mathbf{u}^{n+\frac{1}{2}})_h\right) + h^2(G(\mathbf{u}^{n+\frac{1}{2}}),\mathbf{1})_h, \tag{16}$$

where $(\cdot,\cdot)_h$ is the l_2 discrete inner product and $\mathbf{1} = (1,1,\cdots,1)^T$. And then as will be shown in the following theorem.

Theorem 3.1. *The discrete global energy of the scheme* (14) *satisfies*

$$|H_h^{n+1} - H_h^0| \le C\tau^2.$$

Proof. The scheme (14) is equivalent to the following one by eliminating the value

$$\frac{u_l^{n+1} - 2u^n + u_l^{n-1}}{\tau^2} - \frac{1}{2}D_2^{\alpha}(\mathbf{u}^{n+\frac{1}{2}} + \mathbf{u}^{n-\frac{1}{2}})_l + \frac{1}{2}\left(G'(u_l^{n+\frac{1}{2}}) + G'(u_l^{n-\frac{1}{2}})\right) = 0. \tag{17}$$

Then taking the discrete inner products of above the equation with $2(u_{lm}^{n+\frac{1}{2}} - u_{lm}^{n-\frac{1}{2}})$ and (16), one obtains

$$\begin{aligned}
&|H_h^{n+\frac{1}{2}} - H_h^{n-\frac{1}{2}}| \\
&= \left|\frac{h^2}{2}\left(G'(\mathbf{u}^{n+\frac{1}{2}}) + G'(\mathbf{u}^{n-\frac{1}{2}}), \mathbf{u}^{n+\frac{1}{2}} - \mathbf{u}^{n-\frac{1}{2}}\right)_h + h^2(G(\mathbf{u}^{n+\frac{1}{2}}) - G(\mathbf{u}^{n-\frac{1}{2}}),\mathbf{1})_h\right| \\
&= h^2\left|\sum_{l=0}^{N_x-1}\sum_{m=0}^{N_y-1}\left(\int_{u_{lm}^{n-\frac{1}{2}}}^{u_{lm}^{n+\frac{1}{2}}} G'(u)du - \frac{1}{2}\left(G'(u_{lm}^{n+\frac{1}{2}}) + G'(u_{lm}^{n-\frac{1}{2}})\right)(u_{lm}^{n+\frac{1}{2}} - u_{lm}^{n-\frac{1}{2}})\right)\right| \\
&\le h^2\left|\sum_{l=0}^{N_x-1}\sum_{m=0}^{N_y-1}\left(G''(\zeta)(u_{lm}^{n+\frac{1}{2}} - u_{lm}^{n-\frac{1}{2}})^2\right)\right| \\
&\le \left|Ch^2\sum_{l=0}^{N_x-1}\sum_{m=0}^{N_y-1}\tau^2\right| \le C(b-a)^2\tau^2.
\end{aligned}$$

Therefore, $|H_h^{n+1} - H_h^0| \le \tau\sum_{j=0}^{n}|H_h^{j+1} - H_h^j| \le C\tau^2$. □

Remark 3.2. *It is worth mentioning that the symplectic scheme* (14) *is separable Hamiltonian system, and takes* $H_h(\mathbf{u},\mathbf{v}) = A_h(\mathbf{u}) + B_h(\mathbf{v})$, $A_h(\mathbf{u}) = -\frac{1}{2}\mathbf{u}^T D_2^{\alpha}\mathbf{u} + \sum_{l=0}^{N_x-1}\sum_{m=0}^{N_y-1} G(u_{lm})$, $B_h(v) = \frac{1}{2}\mathbf{v}^T\mathbf{v}$, *then system* (13) *has the following s-stage symplectic integrators*

$$\begin{cases} \mathbf{u}^{(i+1)} = \mathbf{u}^{(i)} + \tau c_i \frac{\partial B_h}{\partial \mathbf{v}}(\mathbf{v}^{(i)}), \\ \mathbf{v}^{(i+1)} = \mathbf{v}^{(i)} - \tau d_i \frac{\partial A_h}{\partial \mathbf{u}}(\mathbf{u}^{(i+1)}), \end{cases} \tag{18}$$

where $i = 1,2,\cdots,s$, $u^{(1)} = u^n$, $u^{(s)} = u^{n+1}$, $v^{(1)} = v^n$, $v^{(s)} = v^{n+1}$ *and* c_i, d_i *are constants which are determined by the order of the system* (18). *They satisfy the full-discrete symplectic conservation law* (15) *and have discrete global energy errors as well.*

3.2. *Multi-symplectic discretization method*

Now applying the Fourier pseudospectral method to the multi-symplectic system (6), one obtains

$$\begin{cases} -\frac{dv_{lm}}{dt} + ({}_{1x}D^{\alpha}\mathbf{w}_1)_{lm} + ({}_{1y}D^{\alpha}\mathbf{w}_2)_{lm} = G'(u_{lm}), \\ \frac{du_{lm}}{dt} = v_{lm}, \\ -({}_{1x}D^{\alpha}\mathbf{u})_{lm} = -w_{1_{lm}}, \\ -({}_{1y}D^{\alpha}\mathbf{u})_{lm} = -w_{2_{lm}}, \end{cases} \tag{19}$$

where $l = 0, \cdots, N_x - 1$, $m = 0, \cdots, N_y - 1$. The system (19) satisfies the following semi-discrete multi-symplectic conservation laws

$$\frac{d}{dt}\omega_{lm} + dz_{lm} \wedge K_1 \mathcal{L}_{hx} dz_{lm} + dz_{lm} \wedge K_2 \mathcal{L}_{hy} dz_{lm} = 0, \quad 0 \le l \le N_x - 1,\ 0 \le m \le N_y - 1, \tag{20}$$

with $z_{lm} = (u_{lm}, v_{lm}, w_{lm})^T$, where

$$\omega_{lm} = \frac{1}{2} dz_{lm} \wedge M dz_{lm}, \ \ \mathcal{L}_{hx} dz_{lm} = \sum_{j=0}^{N_x-1} \sum_{k=0}^{N_y-1} ({}_{1x}D^{\alpha})_{ljkm} dz_{jk}, \ \ \mathcal{L}_{hy} dz_{lm} = \sum_{j=0}^{N_x-1} \sum_{k=0}^{N_y-1} ({}_{1y}D^{\alpha})_{ljkm} dz_{jk}.$$

Owing to ${}_{1x}D^{\alpha}$ and ${}_{1y}D^{\alpha}$ are skew-symmetric matrices, one can sum (20) over l, m and obtain

$$\frac{d}{dt} \sum_{l=0}^{N_x-1} \sum_{m=0}^{N_y-1} \omega_{lm} = \sum_{l=0}^{N_x-1} \sum_{m=0}^{N_y-1} (du_{lm} \wedge dv_{lm}) = 0,$$

which implies the semi-discrete global symplectic conservation law. Thus it is natural to adopt symplectic integrators to integrate the system (19). The implicit midpoint scheme is chosen

$$\begin{cases} -\frac{v_{lm}^{n+1} - v_{lm}^{n}}{\tau} + ({}_{1x}D^{\alpha}\mathbf{w}_1^{n+\frac{1}{2}})_{lm} + ({}_{1y}D^{\alpha}\mathbf{w}_2^{n+\frac{1}{2}})_{lm} = G'(u_{lm}^{n+\frac{1}{2}}), \\ \frac{u_{lm}^{n+1} - u_{lm}^{n}}{\tau} = v_{lm}^{n+\frac{1}{2}}, \\ -({}_{1x}D^{\alpha}\mathbf{u}^{n+\frac{1}{2}})_{lm} = -w_{1_{lm}}^{n+\frac{1}{2}}, \\ -({}_{1y}D^{\alpha}\mathbf{u}^{n+\frac{1}{2}})_{lm} = -w_{2_{lm}}^{n+\frac{1}{2}}, \end{cases} \tag{21}$$

where $\mathbf{w} = (w_1, \cdots, w_{N-1})^T$.

Theorem 3.3. *The scheme* (21) *has following full-discrete multi-symplectic conservation laws*

$$\frac{\omega_{lm}^{n+1} - \omega_{lm}^{n}}{\tau} + dz_{lm}^{n+\frac{1}{2}} \wedge K_1 \mathcal{L}_{hx} dz_{lm}^{n+\frac{1}{2}} + dz_{lm}^{n+\frac{1}{2}} \wedge K_2 \mathcal{L}_{hy} dz_{lm}^{n+\frac{1}{2}} = 0, \quad 0 \le l \le N_x - 1,\ 0 \le m \le N_y - 1,$$

where

$$\omega_{lm}^{n} = \frac{1}{2} dz_{lm}^{n} \wedge M dz_{lm}^{n}, \ \ \mathcal{L}_{hx} dz_{lm}^{n+\frac{1}{2}} = \sum_{j=0}^{N_x-1} \sum_{k=0}^{N_y-1} ({}_{1x}D^{\alpha})_{ljkm} dz_{jk}, \ \ \mathcal{L}_{hy} dz_{lm}^{n+\frac{1}{2}} = \sum_{j=0}^{N_x-1} \sum_{k=0}^{N_y-1} ({}_{1y}D^{\alpha})_{ljkm} dz_{jk}.$$

Proof. Firstly the scheme (21) is rewritten into the compact form

$$M \frac{z_{lm}^{n+1} - z_{lm}^{n}}{\tau} + K_1 \sum_{j=0}^{N_x-1} \sum_{k=0}^{N_y-1} ({}_{1x}D^{\alpha})_{ljkm} z_{jk} + K_2 \sum_{j=0}^{N_x-1} \sum_{k=0}^{N_y-1} ({}_{1y}D^{\alpha})_{ljkm} z_{jk} = \nabla_z S(z_{lm}^{n+\frac{1}{2}}),$$

and the variational equation associated with (21)

$$M \frac{dz_{lm}^{n+1} - dz_{lm}^{n}}{\tau} + K_1 \sum_{j=0}^{N_x-1} \sum_{k=0}^{N_y-1} ({}_{1x}D^{\alpha})_{ljkm} dz_{jk} + K_2 \sum_{j=0}^{N_x-1} \sum_{k=0}^{N_y-1} ({}_{1y}D^{\alpha})_{ljkm} dz_{jk} = S_{zz}(z_{lm}^{n+\frac{1}{2}}) dz_{lm}^{n+\frac{1}{2}}. \tag{22}$$

In fact,

$$dz_{lm}^{n+\frac{1}{2}} \wedge S_{zz}(z_{lm}^{n+\frac{1}{2}}) dz_{lm}^{n+\frac{1}{2}} = 0,$$

so taking the wedge product of (22) with $dz_{lm}^{n+\frac{1}{2}}$

$$\frac{\omega_{lm}^{n+1} - \omega_{lm}^{n}}{\tau} + dz_{lm}^{n+\frac{1}{2}} \wedge K_1 \mathcal{L}_{hx} dz_{lm}^{n+\frac{1}{2}} + dz_{lm}^{n+\frac{1}{2}} \wedge K_2 \mathcal{L}_{hy} dz_{lm}^{n+\frac{1}{2}} = 0,$$

which means the multi-symplectic conservation law. □

So the method is referred to as a multi-symplectic Fourier pseudospectral method. What's more, for the discrete momentum, as will be shown in the following theorem.

Theorem 3.4. *The scheme* (21) *satisfies full-discrete local momentum conservation law in each of the sub-direction*

$$\delta_t I^n_{x_{lm}} + (\mathcal{L}_{hx} V_x^{n+\frac{1}{2}})_{lm} + (\mathcal{L}_{hy} \widetilde{V_{xy}^{n+\frac{1}{2}}})_{lm} = 0,$$
$$\delta_t I^n_{y_{lm}} + (\mathcal{L}_{hy} V_y^{n+\frac{1}{2}})_{lm} + (\mathcal{L}_{hx} \widetilde{V_{yx}^{n+\frac{1}{2}}})_{lm} = 0,$$

where

$$\delta_t I^n_{x_{lm}} = \frac{I^{n+1}_{x_{lm}} - I^n_{x_{lm}}}{\tau},\ \ \delta_t I^n_{y_{lm}} = \frac{I^{n+1}_{y_{lm}} - I^n_{y_{lm}}}{\tau},\ \ I^n_{x_{lm}} = \frac{1}{2}(z^n_{lm})^T M({}_{1x}D^\alpha z^n)_{lm},\ \ I^n_{y_{lm}} = \frac{1}{2}(z^n_{lm})^T M({}_{1y}D^\alpha z^n)_{lm},$$

$$\begin{aligned}(\mathcal{L}_{hx} V_x^{n+\frac{1}{2}})_{lm} = {} & ({}_{1x}D^\alpha z^{n+\frac{1}{2}})^T_{lm} \nabla_z S(z^{n+\frac{1}{2}}_{lm}) - \frac{1}{2}\Big(({}_{1x}D^\alpha z^{n+\frac{1}{2}})^T_{lm} M \delta_t z^n_{lm} + (z^{n+\frac{1}{2}}_{lm})^T M \delta_t ({}_{1x}D^\alpha z^n)_{lm}\Big)\\ & - \frac{1}{2}\Big(({}_{1x}D^\alpha z^{n+\frac{1}{2}})^T_{lm} K_2 ({}_{1y}D^\alpha z^{n+\frac{1}{2}})_{lm} + (z^{n+\frac{1}{2}}_{lm})^T K_2 \delta_t ({}_{1x}D^\alpha {}_{1y}D^\alpha z^n)_{lm}\Big),\end{aligned}$$

$$\begin{aligned}(\mathcal{L}_{hy} V_y^{n+\frac{1}{2}})_{lm} = {} & ({}_{1y}D^\alpha z^{n+\frac{1}{2}})^T_{lm} \nabla_z S(z^{n+\frac{1}{2}}_{lm}) - \frac{1}{2}\Big(({}_{1y}D^\alpha z^{n+\frac{1}{2}})^T_{lm} M \delta_t z^n_{lm} + (z^{n+\frac{1}{2}}_{lm})^T M \delta_t ({}_{1y}D^\alpha z^n)_{lm}\Big)\\ & - \frac{1}{2}\Big(({}_{1y}D^\alpha z^{n+\frac{1}{2}})^T_{lm} K_1 ({}_{1y}D^\alpha z^{n+\frac{1}{2}})_{lm} + (z^{n+\frac{1}{2}}_{lm})^T K_1 \delta_t ({}_{1y}D^\alpha {}_{1x}D^\alpha z^n)_{lm}\Big),\end{aligned}$$

$$(\mathcal{L}_{hy} \widetilde{V_{xy}^{n+\frac{1}{2}}})_{lm} = \frac{1}{2}\Big(({}_{1y}D^\alpha z^{n+\frac{1}{2}})^T_{lm} K_2 \delta_t ({}_{1x}D^\alpha z^n)_{lm} + (z^{n+\frac{1}{2}}_{lm})^T K_2 \delta_t ({}_{1y}D^\alpha {}_{1x}D^\alpha z^n)_{lm}\Big),$$
$$(\mathcal{L}_{hx} \widetilde{V_{yx}^{n+\frac{1}{2}}})_{lm} = \frac{1}{2}\Big(({}_{1x}D^\alpha z^{n+\frac{1}{2}})^T_{lm} K_1 \delta_t ({}_{1x}D^\alpha z^n)_{lm} + (z^{n+\frac{1}{2}}_{lm})^T K_2 \delta_t ({}_{1y}D^\alpha {}_{1x}D^\alpha z^n)_{lm}\Big).$$

Proof. Only prove the local momentum conservation law in the x-axis direction. One first rewrites the scheme (21) into the compact form

$$M\delta_t z^n_{lm} + K_1({}_{1x}D^\alpha z^{n+\frac{1}{2}})_{lm} + K_2({}_{1y}D^\alpha z^{n+\frac{1}{2}})_{lm} = \nabla_z S(z^{n+\frac{1}{2}}_{lm}), \tag{23}$$

(23) is left multiplied by $(D_1^\alpha z^{n+\frac{1}{2}})^T_l$ and K_1 is the skew-symmetric matrix, so

$$({}_{1x}D^\alpha z^{n+\frac{1}{2}})^T_{lm} M \delta_t z^n_{lm} + ({}_{1x}D^\alpha z^{n+\frac{1}{2}})^T_{lm} K_2 ({}_{1y}D^\alpha z^{n+\frac{1}{2}})_{lm} = (D_1^\alpha z^{n+\frac{1}{2}})^T_{lm} \nabla_z S(z^{n+\frac{1}{2}}_{lm}).$$

It is remarkable that

$$\begin{aligned}&({}_{1x}D^\alpha z^{n+\frac{1}{2}})^T_{lm} M \delta_t z^n_{lm}\\ &= \frac{1}{2}({}_{1x}D^\alpha z^{n+\frac{1}{2}})^T_{lm} M \delta_t z^n_{lm} + \frac{1}{2}({}_{1x}D^\alpha z^{n+\frac{1}{2}})^T_{lm} M \delta_t z^n_{lm}\\ &= \frac{1}{2}({}_{1x}D^\alpha z^{n+\frac{1}{2}})^T_{lm} M \delta_t z^n_{lm} - \frac{1}{2}\delta_t\Big((z^n_{lm})^T M ({}_{1x}D^\alpha z^n)_{lm}\Big) + \frac{1}{2}(z^{n+\frac{1}{2}}_{lm})^T M \delta_t ({}_{1x}D^\alpha z^n)_{lm}\\ &= \frac{1}{2}({}_{1x}D^\alpha z^{n+\frac{1}{2}})^T_{lm} M \delta_t z^n_{lm} + \frac{1}{2}(z^{n+\frac{1}{2}}_{lm})^T M \delta_t ({}_{1x}D^\alpha z^n)_{lm} - \delta_t I^n_{lm},\end{aligned}$$

one has

$$\frac{1}{2}({}_{1x}D^\alpha z^{n+\frac{1}{2}})^T_{lm} M \delta_t z^n_{lm} + \frac{1}{2}(z^{n+\frac{1}{2}}_{lm})^T M \delta_t ({}_{1x}D^\alpha z^n)_{lm} - \delta_t I^n_{lm} + + ({}_{1x}D^\alpha z^{n+\frac{1}{2}})^T_{lm} K_2 ({}_{1y}D^\alpha z^{n+\frac{1}{2}})_{lm} = ({}_{1x}D^\alpha z^{n+\frac{1}{2}})^T_{lm} \nabla_z S(z^{n+\frac{1}{2}}_{lm}),$$

which implies

$$\delta_t I^n_{x_{lm}} + (\mathcal{L}_{hx} V_x^{n+\frac{1}{2}})_{lm} + (\mathcal{L}_{hy} \widetilde{V_{xy}^{n+\frac{1}{2}}})_{lm} = 0,$$

the discrete momentum conservation law is obtained. □

Same as the symplectic scheme, the multi-symplectic system preserves discrete multi-symplectic conservation law, on the contrary, it does not preserve energy conservation law in general.

Theorem 3.5. *The discrete global energy of the scheme* (21) *satisfies*

$$|E_h^n - E_h^0| \leq C\tau^2, \tag{24}$$

where $E_h^n = h^2 \sum_{l=0}^{N_x-1} \sum_{m=0}^{N_y-1} E_{lm}^n$, $E_{lm}^n = S(z_{lm}^n) - \frac{1}{2}(z_{lm}^n)^T K_1({}_{1x}D^\alpha z^n)_{lm} - \frac{1}{2}(z_{lm}^n)^T K_2({}_{1y}D^\alpha z^n)_{lm}$.

Proof. Firstly the multi-symplectic scheme (21) is rewritten as the following form

$$M\delta_t z_{lm}^n + K_1({}_{1x}D^\alpha z^{n+\frac{1}{2}})_{lm} + K_2({}_{1y}D^\alpha z^{n+\frac{1}{2}})_{lm} = \nabla_z S(z_{lm}^{n+\frac{1}{2}}).$$

The following equation is obtained by left multiplication $(\delta_t z^n)^T$ of the above equation

$$(\delta_t z_{lm}^n)^T K_1({}_{1x}D^\alpha z^{n+\frac{1}{2}})_{lm} + (\delta_t z_{lm}^n)^T K_2({}_{1y}D^\alpha z^{n+\frac{1}{2}})_{lm} = (\delta_t z_{lm}^n)^T \nabla_z S(z_{lm}^{n+\frac{1}{2}}).$$

It is worth noting that

$$\begin{aligned}
&(\delta_t z_{lm}^n)^T K_1({}_{1x}D^\alpha z^{n+\frac{1}{2}})_{lm} + (\delta_t z_{lm}^n)^T K_2({}_{1y}D^\alpha z^{n+\frac{1}{2}})_{lm} \\
&= \frac{1}{2}\left((\delta_t z_{lm}^n)^T K_1({}_{1x}D^\alpha z^{n+\frac{1}{2}})_{lm} + (\delta_t z_{lm}^n)^T K_2({}_{1y}D^\alpha z^{n+\frac{1}{2}})_{lm}\right) + \frac{1}{2}\left((\delta_t z_{lm}^n)^T K_1({}_{1x}D^\alpha z^{n+\frac{1}{2}})_{lm} + (\delta_t z_{lm}^n)^T K_2({}_{1y}D^\alpha z^{n+\frac{1}{2}})_{lm}\right) \\
&= \frac{1}{2}\left((\delta_t z_{lm}^n)^T K_1({}_{1x}D^\alpha z^{n+\frac{1}{2}})_{lm} + (\delta_t z_{lm}^n)^T K_2({}_{1y}D^\alpha z^{n+\frac{1}{2}})_{lm}\right) - \frac{1}{2}\left((z_{lm}^{n+\frac{1}{2}})^T K_1 \delta_t({}_{1x}D^\alpha z^n)_{lm} + (z_{lm}^{n+\frac{1}{2}})^T K_2 \delta_t({}_{1y}D^\alpha z^n)_{lm}\right) \\
&- \frac{1}{2}\left(({}_{1x}D^\alpha z^{n+\frac{1}{2}})_{lm}^T K_1 \delta_t z_{lm}^n + ({}_{1y}D^\alpha z^{n+\frac{1}{2}})_{lm}^T K_2 \delta_t z_{lm}^n\right) \\
&= \frac{1}{2}\left((\delta_t z_{lm}^n)^T K_1({}_{1x}D^\alpha z^{n+\frac{1}{2}})_{lm} + (\delta_t z_{lm}^n)^T K_2({}_{1y}D^\alpha z^{n+\frac{1}{2}})_{lm}\right) - (F_{\mathbf{x}}^{n+\frac{1}{2}})_{lm}.
\end{aligned}$$

So one has

$$\delta_t S(z_{lm}^n) - (\delta_t z_{lm}^n)^T \nabla_z S(z_{lm}^{n+\frac{1}{2}}) = \delta_t \left(S(z_{lm}^n) - \frac{1}{2}(z_{lm}^n)^T K_1({}_{1x}D^\alpha z^n)_{lm} - \frac{1}{2}(z_{lm}^n)^T K_2({}_{1y}D^\alpha z^n)_{lm}\right) + (F_{\mathbf{x}}^{n+\frac{1}{2}})_{lm}.$$

From the definition of Hamiltonian function $S(z)$ and Taylor expansion formula, one has

$$\begin{aligned}
\delta_t S(z_{lm}^n) - (\delta_t z_{lm}^n)^T \nabla_z S(z^{n+\frac{1}{2}}) &= \frac{u_{lm}^{n+1} - u_{lm}^n}{\tau} G'(u_{lm}^{n+\frac{1}{2}}) - \frac{1}{\tau}\Big(G(u_{lm}^{n+1}) - G(u_{lm}^n)\Big) \\
&= \frac{1}{\tau}\left((G'(u_{lm}^{n+\frac{1}{2}}) - G'(u_{lm}^n))(u_{lm}^{n+1} - u_{lm}^n) + O(\tau^2)\right) \\
&= \frac{1}{\tau}\left(G''(u_{lm}^n)(u_{lm}^{n+1} - u_{lm}^n)^2 + O(\tau^2)\right) \leq C\tau^2.
\end{aligned}$$

Denoting the residual

$$(R_E^{n+\frac{1}{2}})_{lm} = \delta_t E_{lm}^n + (F_{\mathbf{x}}^{n+\frac{1}{2}})_{lm}, \tag{25}$$

one obtains

$$|(R_E^{n+\frac{1}{2}})_{lm}| \leq C\tau^2.$$

And then multiplying (25) with h, summing up for $0 \leq l \leq N_x - 1,\ 0 \leq m \leq N_y - 1$,

$$h^2 \sum_{l=0}^{N_x-1} \sum_{m=0}^{N_y-1} (R_E^{n+\frac{1}{2}})_{lm} = h^2 \sum_{l=0}^{N_x-1} \sum_{m=0}^{N_y-1} (\delta_t E_{lm}^n + (F_{\mathbf{x}}^{n+\frac{1}{2}})_{lm}).$$

Since D_1^α is the skew-symmetry, it holds that $\sum_{l=0}^{N_x-1}\sum_{m=0}^{N_y-1}(F_{\mathbf{x}}^{n+\frac{1}{2}})_{lm}=0$,

$$E_h^n = E_h^0 + h^2\tau\sum_{l=0}^{N_x-1}\sum_{m=0}^{N_y-1}\sum_{j=0}^{N_t-1}(R_E^{j+\frac{1}{2}})_l.$$

Therefore, $|E_h^n - E_h^0| \le C\tau^2$. □

4. Convergence of the scheme

This section presents some basic properties of the Fourier pseudospectral approximation and then rigorously prove convergence for the multi-symplectic Fourier pseudospectral method, accordingly, the convergence analysis of symplectic Fourier pseudospectral method can also be obtained.

For simplicity, one considers $\Omega = (0, 2\pi)\times(0, 2\pi)$. Let $H^r(\Omega)$ be Sobolev space with the norm $\|\cdot\|_r$ and semi-norm $|\cdot|_r$, where $r \ge 0$, and $H_p^r(\Omega)$ be the subspace of $H^r(\Omega)$ consisting of functions being $2\pi-$periodic with derivatives of order up to $r-1$, where the norm and semi-norm as follows.

$$\|u\|_r^2 = \sum_{j,k\in\mathbb{Z}}(1+j^2+k^2)^r|\tilde{u}_{jk}|^2,\quad |u|_r^2 = \sum_{j,k\in\mathbb{Z}}(j^2+k^2)^r|\tilde{u}_{jk}|^2.$$

Denote the interpolation space $\mathcal{J}_N''$ as

$$\mathcal{J}_N'' = \left\{u|u(\mathbf{x}) = \sum_{l_1=-N_x/2}^{N_x/2}\sum_{l_2=-N_y/2}^{N_y/2}\tilde{u}_{l_1l_2}e^{il_1x+il_2y} : \tilde{u}_{N/2,l_2} = \tilde{u}_{-N/2,l_2}, \tilde{u}_{l_1,-N/2} = \tilde{u}_{l_1,N/2}\right\},$$

and $\mathcal{J}_N$ as

$$\mathcal{J}_N = \left\{u|u(\mathbf{x}) = \sum_{l_1=-N_x/2}^{N_x/2}\sum_{l_2=-N_y/2}^{N_y/2}\tilde{u}_{l_1l_2}e^{il_1x+il_2y}\right\}.$$

It is clear that $\mathcal{J}''_N \subseteq \mathcal{J}_N$. Define the orthogonal projection $P_N : L^2(\Omega) \to \mathcal{J}_N$ by

$$(P_Nu - u, \phi) = 0,\quad \forall\phi \in \mathcal{J}_N.$$

Meanwhile, there is a error estimation as follows.

Lemma 4.1. ([21]) *For any $u \in H_p^r(\Omega)$ with $0 \le \sigma \le r$, one has*

$$\|P_Nu - u\|_\sigma \le N^{\mu-s}\|v\|_r,\quad \|P_Nu\|_\sigma \le C\|u\|_\sigma.$$

For $\Phi, \Psi \in \mathcal{J}_N$, one defines the following discrete l^2 inner product and norm:

$$(\Phi,\Psi)_h = \frac{(2\pi)^2}{N_xN_y}\sum_{l=0}^{N_x-1}\sum_{m=0}^{N_y-1}\Phi_{lm}\overline{\Psi}_{lm},\qquad \|\Phi\|_h^2 = (\Phi,\Phi)_h.$$

Lemma 4.2. ([10]) *For any $u \in \mathcal{J}_N''$, $\|u\| \le \|u\|_h \le 2\|u\|$ holds.*

Lemma 4.3. (Gronwall inequality [34]) *Assume that the nonnegative sequences w^n satisfies the following inequality*

$$w^n - w^{n-1} \le A\tau w^n + B\tau w^{n-1} + C_i\tau,$$

where A, B and C_i $(i = 1, 2, \cdots, N_t)$ are nonnegative numbers. Then

$$\max_{1\le n\le N_t} w^n \le \left(w^0 + \tau\sum_{i=1}^{N_t}C_i\right)e^{2(A+B)T}$$

holds, where τ is sufficiently small such that $(A + B)\tau \le (N_t - 1)/(2N_t)$.

For the convenience of writing, some marks are given. Let $z = (u, v, w)^T$ be the exact solution of the multi-symplectic system (6) and $z^n = (\mathbf{u}^n, \mathbf{v}^n, \mathbf{w}^n)^T$ be numerical approximations of the multi-symplectic scheme (21), where $\mathbf{u}^n = (u^n_{00}, \cdots, u^n_{0N_y-1}, \cdots, u^n_{N_x-1N_y-1})$, $\mathbf{v}^n = (v^n_{00}, \cdots, v^n_{0N_y-1}, \cdots, v^n_{N_x-1N_y-1})$, $\mathbf{w}^n = (w^n_{00}, \cdots, w^n_{0N_y-1}, \cdots, w^n_{N_x-1N_y-1})$. And denote $U^n_{lm} = u(x_l, y_m, t_n)$, $V^n_{lm} = v(x_l, y_m, t_n)$, $W^n_{lm} = w(x_l, y_m, t_n)$. Then as will be shown in the following convergence analysis.

Theorem 4.4. *Suppose $u,\ v \in C^3(0, T; H^r_p(\Omega))$, $r > 1$, and $G'' \in L^\infty(\Omega)$. Then there exists a positive constant C, for the scheme* (21),

$$\|u^n - U^n\|_h + \|v^n - V^n\|_h \le C(\tau^2 + N^{-r}).$$

Proof. Denote $z^*_l = (u^*_l, v^*_l, w^*_l)^T$, where $u^* = P_{N-2}u$, $v^* = P_{N-2}v$, $w^* = P_{N-2}w$. The projection of (6) is written as

$$M\partial_t z^* + K_1\mathcal{L}_x z^* + K_2\mathcal{L}_y z^* = P_{N-2}(\nabla_z S(z)),$$

so one has

$$M\partial_t z^{*n+\frac{1}{2}} + K_1\mathcal{L}_x z^{*n+\frac{1}{2}} + K_2\mathcal{L}_y z^{*n+\frac{1}{2}} = P_{N-2}(\nabla_z S(z))^{n+\frac{1}{2}}.$$

Define

$$\eta^n = M\delta_t z^{*n} + K_1\mathcal{L}_x z^{*n+\frac{1}{2}} + K_2\mathcal{L}_y z^{*n+\frac{1}{2}} - P_{N-2}(\nabla_z S(z))^{n+\frac{1}{2}}.$$

Since $z* \in \mathcal{J}''_N$, $\mathcal{L}_{hx} z^{*n+\frac{1}{2}} = {}_{1x}D^\alpha z^{*n+\frac{1}{2}}$,$\mathcal{L}_{hy} z^{*n+\frac{1}{2}} = {}_{1y}D^\alpha z^{*n+\frac{1}{2}}$, one obtains

$$\eta^n = M\delta_t z^{*n} - M\partial_t z^{*n+\frac{1}{2}},$$

that is

$$\eta^n_{1lm} = \delta_t v^{*n}_{lm} - \partial_t v^{*n+\frac{1}{2}}_{lm},$$

$$\eta^n_{2lm} = \delta_t u^{*n}_{lm} - \partial_t u^{*n+\frac{1}{2}}_{lm},$$

where $\eta^n_{lm} = (\eta^n_{1lm}, \eta^n_{2lm})^T$. Using Taylor expansion, it has

$$|\eta^n_{1lm}| = \left|\left(\delta_t v^{*n}_{lm} - \partial_t v^{*n+\frac{1}{2}}_{lm}\right)\right| = \frac{1}{\tau}\left|\left(v^{*n+1}_{l} - v^{*n}_{lm} - \tau\partial_t v^{*n+\frac{1}{2}}_{lm}\right)\right| \le C\tau^2,$$

$$|\eta^n_{2lm}| = \left|\left(\delta_t u^{*n}_{lm} - \partial_t u^{*n+\frac{1}{2}}_{lm}\right)\right| = \frac{1}{\tau}\left|\left(u^{*n+1}_{lm} - u^{*n}_{lm} - \tau\partial_t u^{*n+\frac{1}{2}}_{lm}\right)\right| \le C\tau^2.$$

Therefore,

$$|\eta^n_{lm}| \le C\tau^2. \tag{26}$$

Define $e^n_{lm} = z^{*n}_{lm} - z^n_{lm} = (e^n_{ulm}, e^n_{vlm}, e^n_{wlm})^T$. Subtracting (21) from (26) yields the following error equation

$$\begin{cases} \frac{e^{n+1}_v - e^n_v}{\tau} - {}_{1x}D^\alpha e^{n+\frac{1}{2}}_{w_1} - {}_{1y}D^\alpha e^{n+\frac{1}{2}}_{w_2} = F^{n+\frac{1}{2}} + \eta^n_1, \\ \frac{e^{n+1}_u - e^n_u}{\tau} = e^{n+\frac{1}{2}}_v + \eta^n_2, \\ -{}_{1x}D^\alpha e^{n+\frac{1}{2}}_u = -e^{n+\frac{1}{2}}_{w_1}, \\ -{}_{1y}D^\alpha e^{n+\frac{1}{2}}_u = -e^{n+\frac{1}{2}}_{w_2}, \end{cases} \tag{27}$$

where $F^{n+\frac{1}{2}} = (P_{N-2}G'(u))^{n+\frac{1}{2}} - G'(u^{n+\frac{1}{2}})$. Denoting

$$F^{n+\frac{1}{2}}_{1lm} = (P_{N-2}G'(u))^{n+\frac{1}{2}}_{lm} - G'(u)^{n+\frac{1}{2}}_{lm},\ F^{n+\frac{1}{2}}_{2lm} = G'(u)^{n+\frac{1}{2}}_{lm} - G'(U^{n+\frac{1}{2}}_{lm}),$$

$$F_{3lm}^{n+\frac{1}{2}}=G'(U_{lm}^{n+\frac{1}{2}})-G'(u_{lm}^{*n+\frac{1}{2}}),\quad F_{4lm}^{n+\frac{1}{2}}=G'(u_{lm}^{*n+\frac{1}{2}})-G'(u_{lm}^{n+\frac{1}{2}}),$$

one has $F_{lm}^{n+\frac{1}{2}}=F_{1lm}^{n+\frac{1}{2}}+F_{2lm}^{n+\frac{1}{2}}+F_{3lm}^{n+\frac{1}{2}}+F_{4lm}^{n+\frac{1}{2}}$.

According to Lemma 4.1 and 4.3, one has

$$\|F_1^{n+\frac{1}{2}}\|_h=\|(P_{N-2}G'(u))^{n+\frac{1}{2}}-G'(u)^{n+\frac{1}{2}}\|_h\le CN^{-r}. \tag{28}$$

Use Taylor expansion with an integral remainder term at $t=n+\frac{1}{2}$

$$|F_{2lm}^{n+\frac{1}{2}}|=\left|G'(u)_{lm}^{n+\frac{1}{2}}-G'(U_{lm}^{n+\frac{1}{2}})\right|=\frac{1}{2}\left|G'(u)_{lm}^{n+1}+G'(u)_{lm}^{n}-G'(U_{lm}^{n+\frac{1}{2}})\right|\le C\tau^2. \tag{29}$$

Because of $G''\in L^\infty(\Omega)$, the differential mean value theorem and Lemma 4.1 are used

$$|F_{3lm}^{n+\frac{1}{2}}|=\left|G'(U_{lm}^{n+\frac{1}{2}})-G'(u_{lm}^{*n+\frac{1}{2}})\right|\le|G''(\zeta)|\left|U_{lm}^{n+\frac{1}{2}}-u_{lm}^{*n+\frac{1}{2}}\right|\le CN^{-r}. \tag{30}$$

Similarly,

$$|F_{4lm}^{n+\frac{1}{2}}|=\left|G'(u_{lm}^{*n+\frac{1}{2}})-G'(u_{lm}^{n+\frac{1}{2}})\right|\le|G''(\zeta)|\left|u_{lm}^{*n+\frac{1}{2}}-u_{lm}^{n+\frac{1}{2}}\right|\le C|e_{ulm}^{n+\frac{1}{2}}|. \tag{31}$$

Computing the discrete inner product of (27) with $(e_v^{n+\frac{1}{2}},e_u^{n+\frac{1}{2}},e_{w_1}^{n+\frac{1}{2}},e_{w_2}^{n+\frac{1}{2}})^T$, one has

$$\begin{aligned}\frac{\|e_v^{n+1}\|_h^2-\|e_v^n\|_h^2}{2\tau}+\frac{\|e_u^{n+1}\|_h^2-\|e_u^n\|_h^2}{2\tau}&=({}_{1x}D^\alpha e_u^{n+\frac{1}{2}},{}_{1x}D^\alpha e_v^{n+\frac{1}{2}})_h+({}_{1y}D^\alpha e_u^{n+\frac{1}{2}},{}_{1y}D^\alpha e_v^{n+\frac{1}{2}})_h+(e_v^{n+\frac{1}{2}},e_u^{n+\frac{1}{2}})_h\\&\quad-(F^{n+\frac{1}{2}},e_v^{n+\frac{1}{2}})_h+(\eta_1^n,e_v^{n+\frac{1}{2}})_h+(\eta_2^n,e_u^{n+\frac{1}{2}})_h.\end{aligned} \tag{32}$$

The following inequalities use from Cauchy-Schwartz inequality

$$\begin{aligned}&(\eta_1^n,e_v^{n+\frac{1}{2}})_h\le\frac{1}{2}\|\eta_1^n\|_h^2+\frac{1}{8}\|e_v^{n+1}+e_v^n\|_h^2\le\frac{1}{2}\|\eta_1^n\|_h^2+\frac{1}{4}\Big(\|e_v^{n+1}\|_h^2+\|e_v^n\|_h^2\Big),\\&(\eta_2^n,e_u^{n+\frac{1}{2}})_h\le\frac{1}{2}\|\eta_2^n\|_h^2+\frac{1}{8}\|e_u^{n+1}+e_u^n\|_h^2\le\frac{1}{2}\|\eta_2^n\|_h^2+\frac{1}{4}\Big(\|e_u^{n+1}\|_h^2+\|e_u^n\|_h^2\Big),\\&(F_1^{n+\frac{1}{2}}+F_2^{n+\frac{1}{2}}+F_3^{n+\frac{1}{2}},e_v^{n+\frac{1}{2}})_h\le\frac{1}{2}\Big(\|F_1^{n+\frac{1}{2}}\|_h^2+\|F_2^{n+\frac{1}{2}}\|_h^2+\|F_3^{n+\frac{1}{2}}\|_h^2\Big)+\frac{1}{4}\Big(\|e_v^{n+1}\|_h^2+\|e_v^n\|_h^2\Big),\\&(F_4^{n+\frac{1}{2}},e_v^{n+\frac{1}{2}})_h\le C\Big(\|e_u^n\|_h^2+\|e_u^{n+1}\|_h^2+\|e_v^n\|_h^2+\|e_v^{n+1}\|_h^2\Big),\\&(e_u^{n+\frac{1}{2}},e_v^{n+\frac{1}{2}})_h\le C\Big(\|e_u^n\|_h^2+\|e_u^{n+1}\|_h^2+\|e_v^n\|_h^2+\|e_v^{n+1}\|_h^2\Big),\\&({}_{1x}D^\alpha e_u^{n+\frac{1}{2}},{}_{1x}D^\alpha e_v^{n+\frac{1}{2}})_h\le C\|e_u^{n+\frac{1}{2}}\|_h\|e_v^{n+\frac{1}{2}}\|_h\le C\Big(\|e_u^n\|_h^2+\|e_u^{n+1}\|_h^2+\|e_v^n\|_h^2+\|e_v^{n+1}\|_h^2\Big),\\&({}_{1y}D^\alpha e_u^{n+\frac{1}{2}},{}_{1y}D^\alpha e_v^{n+\frac{1}{2}})_h\le C\|e_u^{n+\frac{1}{2}}\|_h\|e_v^{n+\frac{1}{2}}\|_h\le C\Big(\|e_u^n\|_h^2+\|e_u^{n+1}\|_h^2+\|e_v^n\|_h^2+\|e_v^{n+1}\|_h^2\Big),\end{aligned}$$

where the Plancherel theorem has been used to derived the last inequality. Then substituting (26), (28), (29), (30) and (31) into (32) yields

$$\begin{aligned}\frac{\|e_v^{n+1}\|_h^2-\|e_v^n\|_h^2}{2\tau}+\frac{\|e_u^{n+1}\|_h^2-\|e_u^n\|_h^2}{2\tau}&\le C\Big(\|e_u^n\|_h^2+\|e_u^{n+1}\|_h^2+\|e_v^n\|_h^2+\|e_v^{n+1}\|_h^2\Big)\\&\quad-\frac{1}{2}\Big(\|F_1^{n+\frac{1}{2}}\|_h^2+\|F_2^{n+\frac{1}{2}}\|_h^2+\|F_3^{n+\frac{1}{2}}\|_h^2+\|\eta_1^n\|_h^2+\|\eta_2^n\|_h^2\Big)\\&\le C\Big(\|e_u^n\|_h^2+\|e_v^n\|_h^2+\|e_u^{n+1}\|_h^2+\|e_v^{n+1}\|_h^2\Big)+C(\tau^4+N^{-2r}).\end{aligned}$$

Denoting $w^n = \|e_u^{n+1}\|_h^2 + \|e_v^{n+1}\|_h^2$ and using Lemma 4.3, for a sufficiently small τ,

$$\|e_v^n\|_h^2 + \|e_u^n\|_h^2 \leq \Big(\|e_v^0\|_h^2 + \|e_u^0\|_h^2 + CT(\tau^4 + N^{-2r})\Big).$$

Noting that

$$\|e_v^0\|_h = \|v^{*0} - V^0\|_h \leq CN^{-r},$$

$$\|e_u^0\|_h = \|u^{*0} - U^0\|_h \leq CN^{-r},$$

thus,

$$\|e_v^n\|_h + \|e_u^n\|_h \leq C(\tau^2 + N^{-r}). \tag{33}$$

Then using Lemma 4.1 and (33), we have

$$\begin{aligned}\|u^n - U^n\|_h + \|v^n - V^n\|_h &\leq \|U^n - u^{*n}\|_h + \|u^{*n} - u^n\|_h + \|V^n - v^{*n}\|_h + \|v^{*n} - v^n\|_h \\ &\leq C(\tau^2 + N^{-r}).\end{aligned}$$

Therefore, the theorem is confirmed. □

Similarly, for the symplectic Fourier pseudospectral scheme (14), a similar convergence theorem can also be obtained.

Theorem 4.5. *Suppose $u,\ v \in C^3(0, T; H_p^r(\Omega)),\ \ r > 1$, and $G'' \in L^\infty(\Omega)$. Then there exists a positive constant C, for the scheme* (14),

$$\|u^n - U^n\|_h + \|v^n - V^n\|_h \leq C(\tau^2 + N^{-r}).$$

5. Numerical experiments

In this section, several numerical experiments are given to verify the theoretical results. It notices that the symplectic Fourier pseudospectral (SFP) method and multi-symplectic Fourier pseudospectral (MSFP) method are fully implicit, hence we need to solve them by iterative algorithm with iterative tolerance 10^{-13}. First of all, the convergence order formula is given by

$$order = \frac{\log(error_1/error_2)}{\log(2)},$$

where $error_j,\ j = 1, 2$ denote the discrete norm $\|\cdot\|_h$ errors.

Example 5.1. *Considering semi-linear fractional wave equation with periodic boundary conditions*

$$\begin{cases} \partial_{tt}u(x,y,t) + a^2(-\triangle)^{\frac{\alpha}{2}}u(x,y,t) = bu^3(x,y,t) - au(x,y,t), \\ u(x,y,0) = \sqrt{\frac{2a}{b}}\operatorname{sech}(\lambda x)\operatorname{sech}(\lambda y), \\ u_t(x,y,0) = c\lambda\sqrt{\frac{2a}{b}}\operatorname{sech}(\lambda x)\tanh(\lambda x)\operatorname{sech}(\lambda y)\tanh(\lambda y), \\ -20 \leq x \leq 20,\ -20 \leq y \leq 20,\ 0 \leq t \leq T, \end{cases}$$

where $\lambda = \sqrt{a/(a^2 - c^2)}$ and $a,\ b,\ a^2 - c^2 > 0$. And we consider the parameters $a = 0.3,\ b = 1,\ c = 0.25$.

We choose that the numerical exact solution is obtained by $N := N_x = N_y = 512$, $\tau = 0.001$. Convergence orders are also verified in time and space for SFP method and MSFP method. Figure 1 and 2 plot temporal and spatial errors in the log scale at the time $T = 0.5$, respectively. It can be found that convergence orders are of the second-order in time and spatial convergence is spectral accuracy. Furthermore, the energy errors of the SFP method is plotted in Figure 3 when $\tau = 0.01$, $N = 256$. It shows that the global energy errors are $O(\tau^2)$. And then the momentum and its error are plotted in Figure 4. It is found that the momentum is also equal to machine error, approximately zero. It indicates that momentum conservation laws hold. So, they preserve full discrete conservation properties well. Figure 5 and 6 display that the numerical solution and contours use $\tau = 0.01$, $N = 256$ for $T = 2$, with different α. It can be easily seen that the figure on x and y axes decay rapidly. Since two large amount of energy is concentrated in the center of the peak, it has two prominent central wave crest. And the central wave crest becomes thicker and slower with the decrease of α. From the contour map, the distance between two peaks increases with the increase of α and peaks values become smaller. Therefore for the difference of α, it also has a certain influence on the solution.

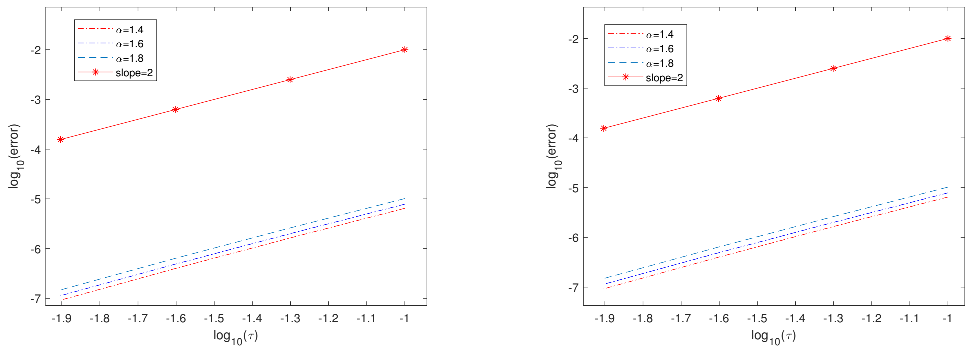

Figure 1: Temporal errors of SFP (left) and MSFP (right) for Example 5.1 with different α at $T = 0.5$.

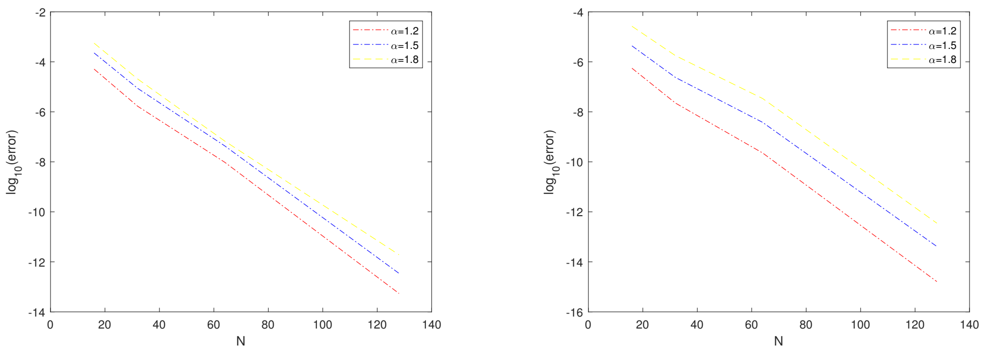

Figure 2: Spatial errors of SFP (left) and MSFP (right) for Example 5.1 with different α at $T = 0.5$.

Example 5.2. *Consider the following two-dimensional fractional sine-Gordon equation*

$$\begin{cases} \partial_{tt}u(x,y,t) + (-\triangle)^{\frac{\alpha}{2}}u(x,y,t) + \sin u(x,y,t) = 0, \\ u_t(x,y,0) = \frac{4}{\sqrt{1+c^2}}\operatorname{sech}\left(\frac{x}{\sqrt{1+c^2}}\right)\operatorname{sech}\left(\frac{y}{\sqrt{1+c^2}}\right), \\ u(x,y,0) = 0, \\ -20 \le x \le 20,\ -20 \le y \le 20,\ 0 \le t \le T, \end{cases}$$

with periodic boundary conditions and $c = 0.5$.

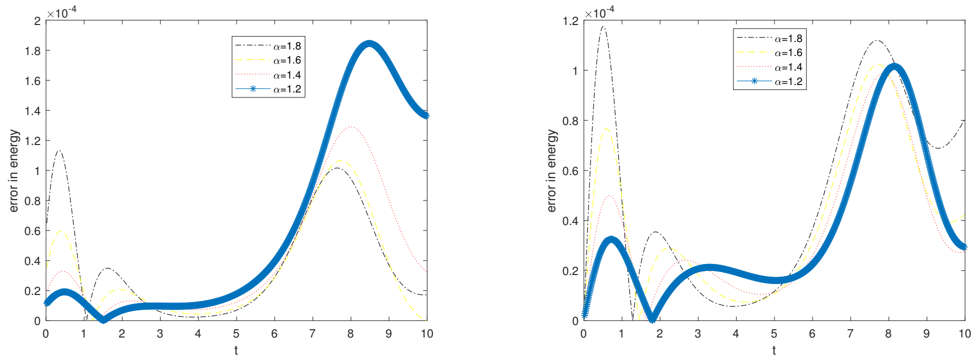

Figure 3: Energy errors of MSFP (left) and SFP (right) for Example 5.1 with different α when $\tau = 0.01$, $N = 256$.

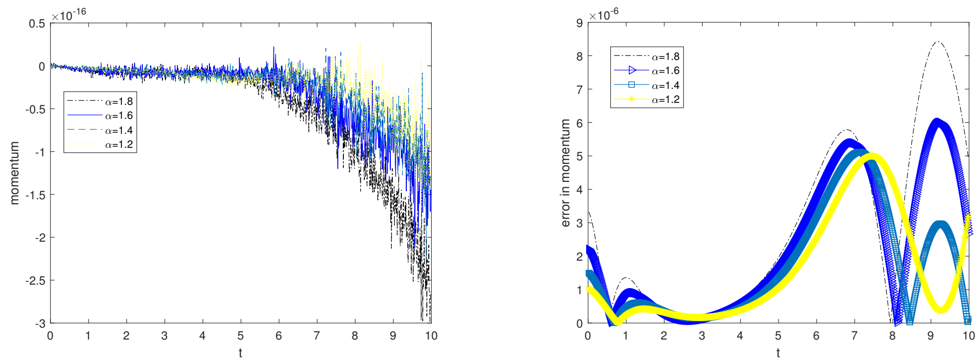

Figure 4: Momentum and momentum errors for Example 5.1 with different α when $\tau = 0.01$, $N = 256$.

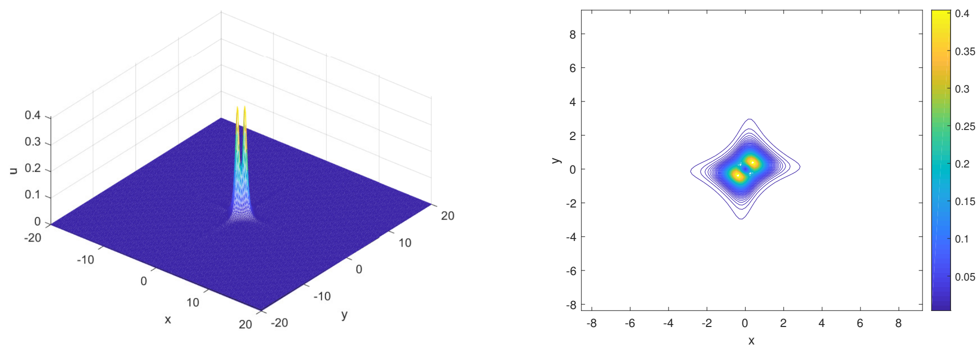

Figure 5: Numerical solution and contours for Example 5.1 with $\alpha = 1.4$ at $T = 2$.

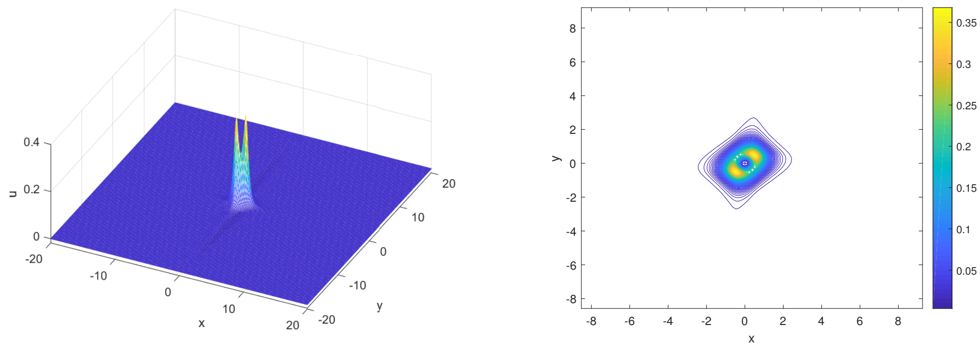

Figure 6: Numerical solution and contours for Example 5.1 with $\alpha = 1.8$ at $T = 2$.

We choose that the numerical exact solution is obtained by $N := N_x = N_y = 512$, $\tau = 0.001$. First, convergence orders are also verified in time and space. Figure 7 plots temporal and spatial errors in the log scale at the time $T = 0.5$, respectively. We found that convergence orders are of the second-order in time and spatial convergence is spectral accuracy. Furthermore, the energy errors is plotted in Figure 8 when $\tau = 0.01$, $N = 256$. It also shows that their global energy errors are oscillatory and bounded, and satisfy $O(\tau^2)$. And then the momentum and its error are plotted in Figure 9. It is also found that the momentum is also equal to machine error. So, they preserve full discrete conservation properties well. Figure 10 displays that the numerical solution use $\tau = 0.01$, $N = 256$ for $T = 2$, with different α. It can be easily seen that the figure on x and y axes are symmetrical and decay rapidly. Since a large amount of energy is concentrated in the center of the peak, it has a prominent central wave crest. And the central wave crest becomes thicker and slower with the increase of α. Therefore for the difference of α, it also has a certain influence on the solution.

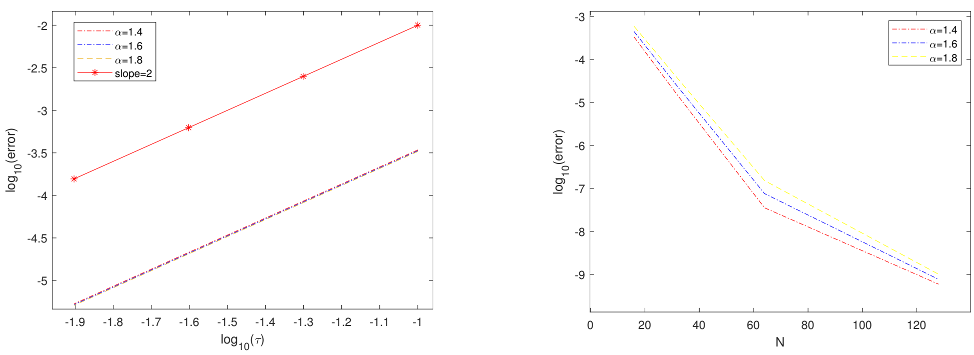

Figure 7: Temporal errors (left) and spatial errors (right) for Example 5.2 with different α at $T = 0.5$.

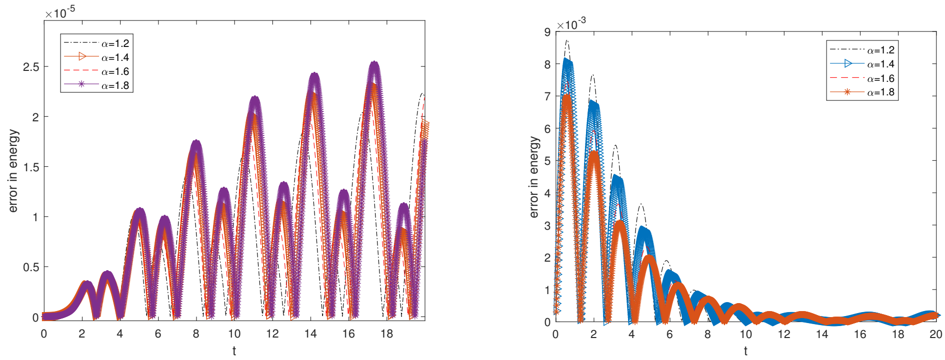

Figure 8: Energy errors of MSFP (left) and SFP (right) for Example 5.2 with different α when $\tau = 0.01$, $N = 256$.

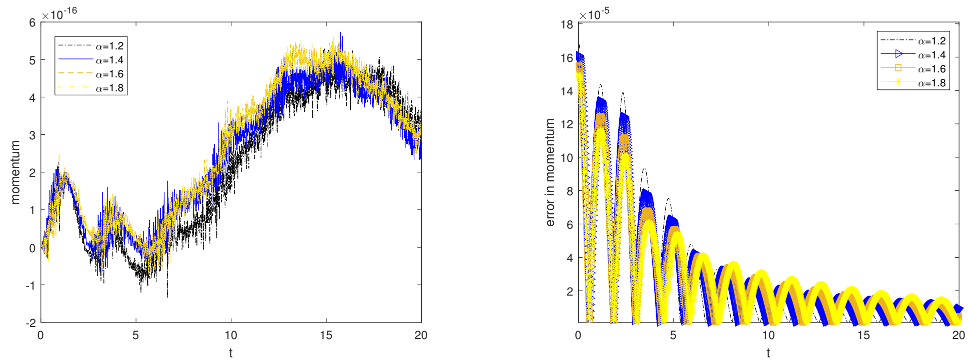

Figure 9: Momentum and momentum errors for Example 5.2 with different α when $\tau = 0.01$, $N = 256$.

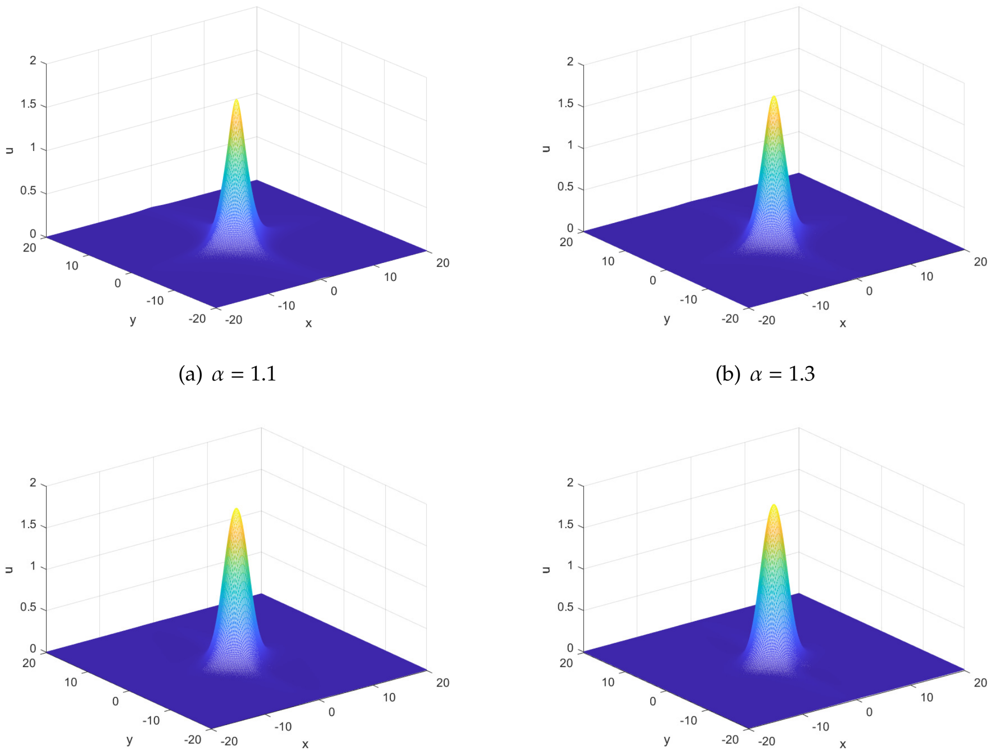

(a) $\alpha = 1.1$ (b) $\alpha = 1.3$

(c) $\alpha = 1.7$ (d) $\alpha = 1.9$

Figure 10: Numerical solutions for Example 5.2 with different α at $T = 2$.

6. Conclusions

This paper investigates structure-preserving numerical methods for the two dimensional nonlinear fractional wave equation and discusses their convergence. According to using the variational principle with fractional Laplace, the equations can be transformed into the Hamiltonian system. Then it is proposed a structure-preserving method with the Fourier pseudospectral method in space and midpoint method in time, and proved the discrete systems satisfy the corresponding conservation laws. Furthermore, one gives a rigorous the energy error analysis of discrete symplectic and multi-symplectic systems. The convergence is discussed in the discrete l^2 norm, and the convergence order is $O(\tau^2 + N^{-r})$. In the end, some examples are given to illustrate the efficiency and accuracy of theoretical results.

Acknowledgments

The authors would like to express their appreciation to the anonymous referees for their many valuable suggestions. And we are also very grateful to the editor for giving the opportunity to further revise the manuscript.

References

[1] Ainsworth, M., and Mao, Z. Analysis and approximation of a fractional Cahn-Hilliard equation. *SIAM J. Numer. Anal. 55*, 4 (2017), 1689–1718.

[2] Bader, P., Blanes, S., Casas, F., and Kopylov, N. Novel symplectic integrators for the Klein-Gordon equation with space- and time-dependent mass. *J. Comput. Appl. Math. 350* (2019), 130–1138.

[3] Chen, C., Hong, J., Sim, C., and Sonwu, K. Energy and quadratic invariants preserving (EQUIP) multi-symplectic methods for Hamiltonian wave equations. *J. Comput. Phys. 418* (2020), 109599.

[4] Chen, J. Symplectic and multisymplectic Fourier pseudospectral discretizations for the Klein-Gordon equation. *Lett. Math. Phys. 75* (2006), 293–305.

[5] Cohen, D., Hairer, E., and Lubich, C. Conservation of energy, momentum and actionsin numerical discretizations of non-linear wave equations. *Numer. Math. 110* (2008), 113–143.

[6] Duncan, D. Symplectic finite difference approximations of the nonlinear Klein-Gordon equation. *SIAM J. Numer. Anal. 34* (1997), 1742–1760.

[7] Fei, M., Huang, C., and Wang, P. Error estimates of structure-preserving Fourier pseudospectral methods for the fractional Schrödinger equation. *Numer. Meth. Part. D. Eq. 36* (2020), 369–393.

[8] Feng, K., and Qin, M. Hamiltonian algorithm for Hamiltonian dynamical systems. *Prog. Nat. Sci. 2*, 1 (1991), 105–116.

[9] Feng, K., and Qin, M. *Symplectic Geometric Algorithms for Hamiltonian Systems*. Springer, Berlin, 2010.

[10] Gong, Y., Wang, Q., Wang, Y., and Cai, J. A conservative Fourier pseudo-spectral method for the nonlinear Schrödinger equation. *J. Comput. Phys. 328* (2017), 354–370.

[11] Hairer, E., Lubich, C., and Wanner, G. *Geometric Numerical Integration: Structure-Preserving Algorithms for Ordinary Differential Equations*. Springer, Berlin, 2006.

[12] Hendy, A., and Macías-Díaz, J. A numerically efficient and conservative model for a Riesz space-fractional Klein-Gordon-Zakharov system. *Commun. Nonlinear Sci. Numer. Simulat. 71* (2019), 22–37.

[13] Hong, J., and Sun, Y. Generating functions of multi-symplectic RK methods via dw Hamilton-Jacobi equations. *Numer. Math. 110* (2008), 491–519.

[14] Jiang, C., Wang, Y., and Cai, W. A linearly implicit energy-preserving exponential integrator for the nonlinear Klein-Gordon equation. *J. Comput. Phys. 419* (2020), DOI: 10.1016/j.jcp.2020.109690.

[15] Kilbas, A., Srivastava, H., and Trujillo, J. *Theory and Applications of Fractional Differential Equations*. Elsevier, Netherlands, 2006.

[16] Lakestani, M., and Dehghan, M. Collocation and finite difference-collocation methods for the solution of nonlinear Klein-Gordon equation. *Comput. Phys. Commun. 181* (2010), 1392–1401.

[17] Mao, Z., and Shen, J. Spectral element method with geometric mesh for two-sided fractional differential equations. *Adv. Comput. Math. 44*, 3 (2018), 745–771.

[18] Qian, X., Fu, H., and Song, S. Structure-preserving wavelet algorithms for the nonlinear Dirac model. *Adv. Appl. Math. Mech. 9*, 4 (2017), 964–989.

[19] Reich, S. Multi-symplectic Runge-Kutta collocation methods for Hamiltonian wave equations. *J. Comput. Phys. 157* (2002), 473–499.

[20] Sanz-Serna, J., and Calvo, M. *Numerical Hamiltonian Problems*. Chapman & Hall, London, 1994.

[21] Shen, J., Tang, T., and Wang, L. *Spectral Method Algorithms, Analysis and Applications*. Spring, Berlin Heidelberg, 2011.

[22] Shi, D., and Wang, R. Unconditional superconvergence analysis of a two-grid finite element method for nonlinear wave equations. *Appl. Numer. Math. 150* (2020), 38–50.

[23] Tu, X., Murua, A., and Tang, Y. New high order symplectic integrators via generating functions with its application in many-body problem. *BIT Numer. Math. 60* (2020), 509–535.

[24] Wang, B., and Wu, X. A symplectic approximation with nonlinear stability and convergence analysis for efficiently solving semi-linear Klein-Gordon equations. *Appl. Numer. Math. 142* (2019), 64–89.

[25] Wang, D., Xiao, A., and Yang, W. Maximumnorm error analysis of a difference scheme for the space fractional CNLS. *Appl. Math. Comput. 257* (2015), 241–251.

[26] Wang, H., Yang, W., and Huang, Y. Adaptive finite element method for the sound wave problems in two kinds of media. *Comput. Math. Appl. 79* (2020), 789–801.

[27] Wang, J. Symplectic-preserving Fourier spectral scheme for space fractional Klein-Gordon-Schrödinger equations. *Numer. Meth. Part. D. Eq. 37* (2021), 1030–1056.

[28] Wang, L., Kong, L., Zhang, L., Zhang, W., and Zheng, X. Multi-symplectic preserving integrator for the Schrödinger equation with wave operator. *Appl. Math. Model. 22*, 39 (2015), 6817–6829.

[29] Wang, P., and Huang, C. Structure-preserving numerical methods for the fractional Schrödinger equation. *Appl. Numer. Math. 129* (2018), 137–158.

[30] Wu, L., Ma, Q., and Ding, X. Conformal structure-preserving method for two-dimensional damped nonlinear fractional schrödinger equation. *Numerical Methods for Partial Differential Equations 39*, 4 (2023), 3195–3221.

[31] Xiao, A., and Wang, J. Symplectic scheme for the Schrödinger equation with fractional laplacian. *Appl. Numer. Math. 146* (2019), 469–487.

[32] Yang, Y., Song, Y., Li, H., and Wang, Y. A new explicit symplectic fourier pseudospectral method for Klein-Gordon-Schrödinger equation. *Adv. Appl. Math. Mech 10*, 1 (2018), 242–260.

[33] Zhang, J., and Kong, L. New energy-preserving schemes for Klein-Gordon-Schrödinger equations. *Appl. Math. Model. 40*, 15-16 (2016), 6969–6982.

[34] Zhou, Y. *Applications of Discrete Functional Analysis to the Finite Difference Method*. International Academic Publishers, Beijing, 1990.